Proceedings of the Korean Nuclear Society Autumn Meeting
Seoul, Korea, October 1998

Evaluation of Neutron and Proton Cross Sections of Al-27 up to 2 GeV

Youngouk LEE, Choong-Sup GIL and Jonghwa CHANG
Korea Atomic Energy Research Institute

Abstract

We evaluated neutron and proton cross sections of Al-27 for energies up to 2 GeV which are important in shielding and structurure for accelerator-driven system and also as monitor reactions. The optical model parameters up to 250 MeV were optimized by ECISPLOT with phenomenological potential form proposed by Chiba. The resulting total, reaction cross section and elastic angular distributions reproduced the experimental data fairly well. The derived transmission coefficients for neutron and proton from the optical models are fed into the GNASH code system to evaluate angle-energy correlated emission spectra for light ejectiles and gamma rays. For energies above 250 MeV up to 2 GeV, the total, reaction cross sections were evaluated by an empirical fit and recent systematics. The nucleon emission spectra including pion were estimated by use of QMD+SDM (Quantum Molecular Dynamics + Statistical Decay Model).

I. Introduction

Nuclear data on conventional thermal and fast reactors mainly consist of neutron induced cross sections in energy below 20 MeV. However, recent new applications such as radiation transport simulations of cancer radiotherapy and the accelerator-driven transmutation of waste require well-tested nuclear data of neutrons and protons above 20 MeV up to a few GeV. This work is aimed to accurately represent integrated cross sections and inclusive emission for aluminium which are important in shielding and structural material for accelerator-driven system and also important as monitor cross sections to measure other material reactions.

Currently some evaluation works are underway to build up high energy libraries for neutron and protons above 20 MeV. As summarized in Table 1 for the evaluation of aluminium, JENDL (Japanese evaluated Nuclear Data Library) High Energy File[1] has incident neutron cross sections for energies up to 50 MeV using Walter-Gauss[2] potential for neutron. LANL (Los Alamos National Laboratory) 150 MeV File[3] has neutron and proton cross sections up to 150 MeV with the optical potential of Petler[4] up to 60 MeV, and above this energy the Madland global potential [5] was used. Intercomparison of these two evaluation data[6] with available measurements showed JENDL needs improvement in the optical model which had been tuned for neutron energies below 20 MeV. LANL applied two different sets of optical models for neutron and proton, giving discontinuities of cross sections at boundary energies. The evaluation method in our work differs from previous works of LANL and JENDL in followings:

- Extend energy range up to 2 GeV, covering recent accelerator power,
- Develop global optical model parameters up to 250 MeV for neutron and proton,
- Apply recent systematics for total and reaction cross sections up to 2 GeV,
- Introduce QMD+SDM for energies above pion production threshold up to 2 GeV.

II. For Energies up to 250 MeV

II.1 Optical models

Evaluation starts with determining global optical model parameters of neutron and proton for aluminium to describe measured total, reaction and elastic scattering cross sections. The potential form factor was chosen to be of Woods-Saxson form for V_r and W_v, derivative Wood-Saxson for W_d and Thomas-Fermi form for spin-orbit parts. We adopted Chiba's potential depths[7] whose energy dependencies of potential depths are expressed in the following way similar to that proposed by Delaroche et al.[8]:

$$V_r(E) = V_0 e^{-\lambda_{Vr}(E-E_f)} + V_1 + V_2 I \qquad r_v(E) = r_{v0} + r_{v1} E \qquad a_v(E) = a_{v0} + a_{v1} E$$

$$W_v(E) = W_{v0} \frac{(E-E_F)^4}{(E-E_f)^4 + W_{v1}^4} \qquad r_{wv}(E) = r_V(E) \qquad a_{wv}(E) = a_v(E)$$

$$W_d(E) = W_{d0} e^{\lambda_{Wd}(E-E_f)} \frac{(E-E_f)^4}{(E-E_f)^4 + W_{d1}^4} \qquad r_{wd}(E) = r_{wd0} + r_{wd1} E \qquad a_{wd}(E) = a_{wd0} + a_{wd1} E$$

$$V_{so}(E) = 6.0 e^{-0.005E} \qquad r_{vso} = 1.017 \qquad a_{vso} = 0.60$$

$$W_{so}(E) = 0.2 - 0.011E \qquad r_{wso} = 1.017 \qquad a_{wso} = 0.60$$

where the Fermi energy E_f for neutron is given by

$$E_f(^N_Z A) = -\frac{1}{2}[S_n(^N_Z A) + S_n(^{N+1}_Z A + 1)]$$

with S_n the neutron separation energy, and for protons by

$$E_f(^N_Z A) = -\frac{1}{2}[S_p(^N_Z A) + S_p(^N_{Z+1} A + 1)]$$

with S_p the proton separation energy.

These energy dependent parameters are globally optimized by ECISPLOT[9], an interactive optical parameter searcher with simulated annealing algorithm, developed by one of authors. It is X-Window based software system incorporated with nuclear reaction code ECIS-96[10]. Table 2 lists finally optimized two sets of potentials for neutron and proton that describe the experimental data. The resulting total cross sections and elastic angular distributions are shown in Figs. 1-4, with various measurements, and compared with JENDL and LANL evaluations up to 250 MeV. Our global optical model parameters give excellent agreement with most of experimental data over entire energy range for both incident neutron and proton.

II.2 Pre-equilibrium and compound reactions

Compound reaction calculations and preequilibrium corrections were performed in the course of the GNASH[11] calculations using the exciton model of Kalbach[12], discrete level data from nuclear data sheets, continuum level densities using the formulation of Ignatyuk[13] and pairing and shell parameters from the Cook[14] analysis. The derived transmission coefficients for neutron and proton from the optical models as well as deuteron, triton and alpha particles are fed into the GNASH to evaluate angle-energy correlated emission spectra for light ejectiles and gamma rays. Besides neutron and proton, following global potentials were also employed in the evaluations for composite particles which are needed for the inverse process of composite particle emission:

Deuterons : Perey and Perey[15]
Tritons : Watanabe[16]
Alphas : Arthur and Young[17]

Gamma-ray transmission coefficients were calculated using the Kopecky-Uhl model[18].

Figures 5 and 6 compares the resulting inclusive cross sections of incident neutron giving residual Na-23 isotope and incident proton giving residual Na-24 isotope against Los Alamos data together with evaluations from LANL and JENDL. Better agreements of our results are partly due to more accurate neutron and proton transmission coefficients determined during global optical model parameter optimization. Figure 7 simply shows emission spectra at 30 degree of 90 Mev (p,xn) reaction compared with measurements and LANL evaluation. It reproduced well the high energy tail of emission spectra from pre-equilibrium emission.

III For Energies up to 2 GeV

III.1 Total and reaction cross sections

Since there are not enough measurements and reliable physics description for total, reaction cross sections and elastic angular distributions above few hundred energies of incident neutron and protons, we

made an empirical fit with available measurements and systematics. For total and reaction cross sections, we applied data fitting combined with recent systematics developed by NASA[19] that describes nucleon induced reaction cross sections up to few GeV. The NASA systematics has following form for the reaction cross section:

$$\sigma_R = \pi r_0^2 \, (A_P^{1/3} + A_T^{1/3} + \delta_E)^2 (1 - \frac{B}{E_{cm}})$$

where r_0 = 1.1 fm, and E_{cm} is the colliding system center of mass energy in MeV. Details of parameters δ_E (Pauli blocking factor) and B (energy-dependent Coulomb interaction barrier) are explained in the reference[19]. These evaluations are merged with the cross sections obtained from optical model approach.

Figure 8 and 9 shows evaluated total and reaction cross sections up to 2 GeV, reproducing measured data quite well, except mismatches in the energies around 400 MeV for neutron total cross sections. It is considered that the total cross section data for those energy region have larger errors than reported, so our evaluation eliminated those data when fitting.

III.2 Emission of nucleons

For energies above pion production threshold, we tried QMD+SDM[20] instead of well-known INC(Intra Nuclear Cascade) model to calculate nucleon emission spectra. This model is based on quantum molecular dynamics (QMD) incorporated with a statistical decay model(SDM) to describe various nuclear reaction in a unified way. INC and pre-equilibrium processes are described by QMD model, and equilibrium process by SDM. Recent publications showed that this model reproduced the overall features of the outgoing particles (neutron, proton and pion) quite well without assuming any reaction mechanism, and without changing the parameter set. Despite the fact that this code system is considered to be immature for the actual production work, we tried calculations of nucleon emission spectra for incident neutron and proton of energies above 150 MeV up 2 GeV. One of our results, neutron emission spectra for the reaction p(585 MeV) + Al-27 at different laboratory angles is shown in Fig. 10. reproducing measured data quite well in all emission angles.

IV. Summary

We evaluated the neutron and proton cross sections of Al-27 which is important in shielding and structural material for accelerator-driven system for energies up to 2 GeV. The characteristics of our evaluation method are :

- Energy range up to 2 GeV, covering recent accelerator power,
- Global optical model parameters up to 250 MeV for neutron and proton,
- Recent systematics for total and reaction cross sections above 250 MeV up to 2 GeV,
- Use of QMD+SDM for energies above pion production threshold up to 2 GeV.

Optimized potential parameters describes well the experimental data of total, reaction cross section and elastic angular distributions. The resulting transmission coefficients of neutron and proton are fed into the GNASH code to evaluate angle-energy correlated emission spectra for light ejectiles with A≤4 and gamma rays. Some of inclusive cross sections from GNASH caculations were compared with experimental data, giving good agreements. For energies above 250 MeV up to 2 GeV, the total and reaction cross sections were evaluated by an empirical fit and recent systematics. The neutron, proton and pion emission spectra for energies above pion production threshold energy were estimated by use of QMD+SDM.

V. Acknowledgement

We gratefully acknowdge usefull discussions with S. Chiba. This work was performed under the auspices of Korea Ministry of Science and Technology as one of long-term nuclear R&D programs.

References

[1] T. Fukahori and S. Chiba, "Status of Nuclear Data Evaluation for JENDL High Energy File", The 2nd Specialists' Meeting on High Energy Nuclear Data, Tokai, Japan, Jan. 26-27 (1995)

[2] R.L. Walter and P.P. Gauss, "A Global Optical Potential Model for Neutron Scattering for A>53 and

10 MeV < E < 80 MeV", Proc. Int. Conf. Nuclear Data for basic and Applied Science, Santa Fe, New Mexico, p.1079 (1985)
[3] M.B. Chadwick, P.G. Young, and R.E. MacFarlane, "The Los Alamos 150 MeV Library", private communication (1997)
[4] J. S. Petler, M. S. Islam, and R. W. Finlay, "Microscopic Optical Model Analysis of Nucleon Scattering from Light Nuclei", Phys. Rev. **C32**, 673 (1985).
[5] D.G. Madland, "Proceedings of a Specialists's Meeting on Preequilibrium Reactions", Semmering, Austria, 10-12 Feb. 1988, NEANDC-245, p.103 (1988)
[6] Y. Lee and T. Fukahori, "Intercomparison of High Energy Files", The 3nd Specialists' Meeting on High Energy Nuclear Data, Tokai, Japan, Mar. 30-31 (1998)
[7] S. Chiba, private communication
[8] J.P. Delaroche, Y. Wang and J. Rapaport, Phys. Rev. **C39**, 391 (1989)
[9] Y. Lee et al, "ECISPLOT: Interactive Optical Model Searcher with Simulated Annealing Algorithm", will be published.
[10] J. Raynal, Notes on ECIS94, CEA Saclay report CEA-N-2772 (1994)
[11] P. G. Young, E. D. Arthur, and M. B. Chadwick, "Comprehensive Nuclear Model Calculations: Introduction to the Theory and Use of the GNASH Code," LA-12343-MS (1992).
[12] C. Kalbach, "Systematics of Continuum Angular Distributions: Extensions to Higher Energies," Phys. Rev. **C37**, 2350 (1988)
[13] A. V. Ignatyuk, G. N. Smirenkin, and A. S. Tishin,"Phenomenological Description of the Energy Dependence of the Level Density Parameter", Sov. J. Nucl. Phys. 21, 255 (1975).
[14]. J. L. Cook, H. Ferguson, and A. R. Musgrove, "Nuclear Level Densities in Intermediate and Heavy Nuclei", Aust. J. Phys. 20, 477 (1967).
[15] C. M. Perey and F. G. Perey, Phys. Rev. **132**, 755 (1963)
[16] F.D. Becchetti, Jr., and G.W. Greenlees in "Polarization Phenomena in Nuclear Reactions", (Ed: H.H. Barschall and W. Haeberli, The University of Wisconsin Press,1971) p.682.
[17]. J. Kopecky and M. Uhl, "Test of Gamma-Ray Strength Functions in Nuclear Reaction Model Calculations", Phys. Rev. **C42**, 1941 (1990).
[18] P.G. Young, IAEA INDC(NDS)-335 p.109 (1995)
[19] R.K. Tripathi et al, "Universal Parameterization of Absorption Cross Sections" , NASA Technical Paper 3621, Jan. 1997.
[20] K. Niita et al., Phys. Rev., **C52**, 2620 (1995)

Table 1. Comparison of Evaluation Methods adopted for aluminium above 20 MeV

	yr	E_{max}(MeV)	Optical Model	Decaying Process
JENDL HE	96	50	n: Walter-Gauss	Exciton + HF theory
LANL-150	97	150	n,p: Petler + Madland	Exciton+MPE+HF theory(FKK for validation)
This Work		2000	n,p: Chiba (< 250 MeV) Systematics (< 2GeV)	Exciton+MPE+HF theory (< 250MeV) QMD+SDM (< 2000 MeV)

Table 2. Optical potential parameters for n,p + Al-27 interaction up to 250 MeV

	V_0	λ_{vr}	V_1	V_2	r_{v0}	r_{v1}	a_{v0}	a_{v1}
Neutron	109.8	0.006	-48.27	0.168	1.19	0.00013	0.627	0.0004
Proton	162.58	0.0095	-78.53	0.419	1.153	0.00016	0.552	0.0016

	W_{v0}	W_{v1}	λ_{v1}	W_{d0}	W_{d1}	r_{wd0}	r_{wd1}	a_{wd0}	a_{wd1}
neutron	10.58	41.50	0.06512	46.50	18.32	1.06	0.0	0.62	0.0008
proton	10.89	35.86	0.057	38.91	28.09	1.3	0.0	0.60	0.0

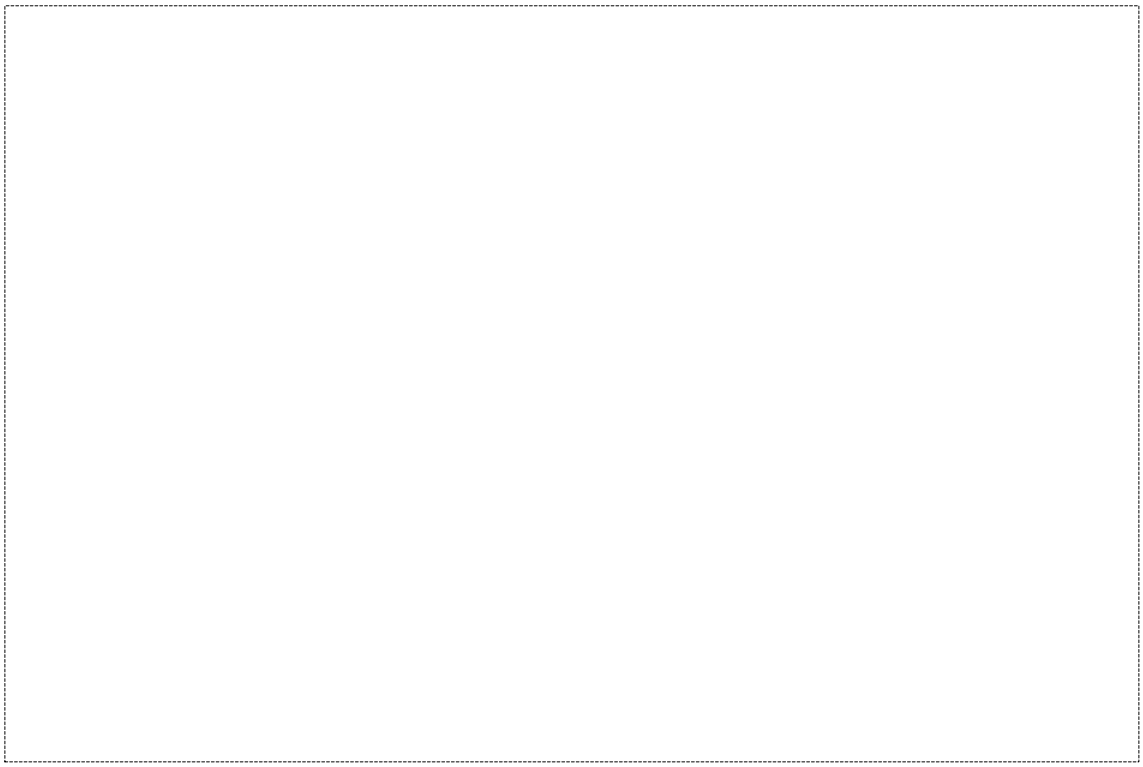

Fig. 1. Total cross sections of neutron for aluminium from optimized optical potential parameters compared with measurements for energies up to 250 MeV

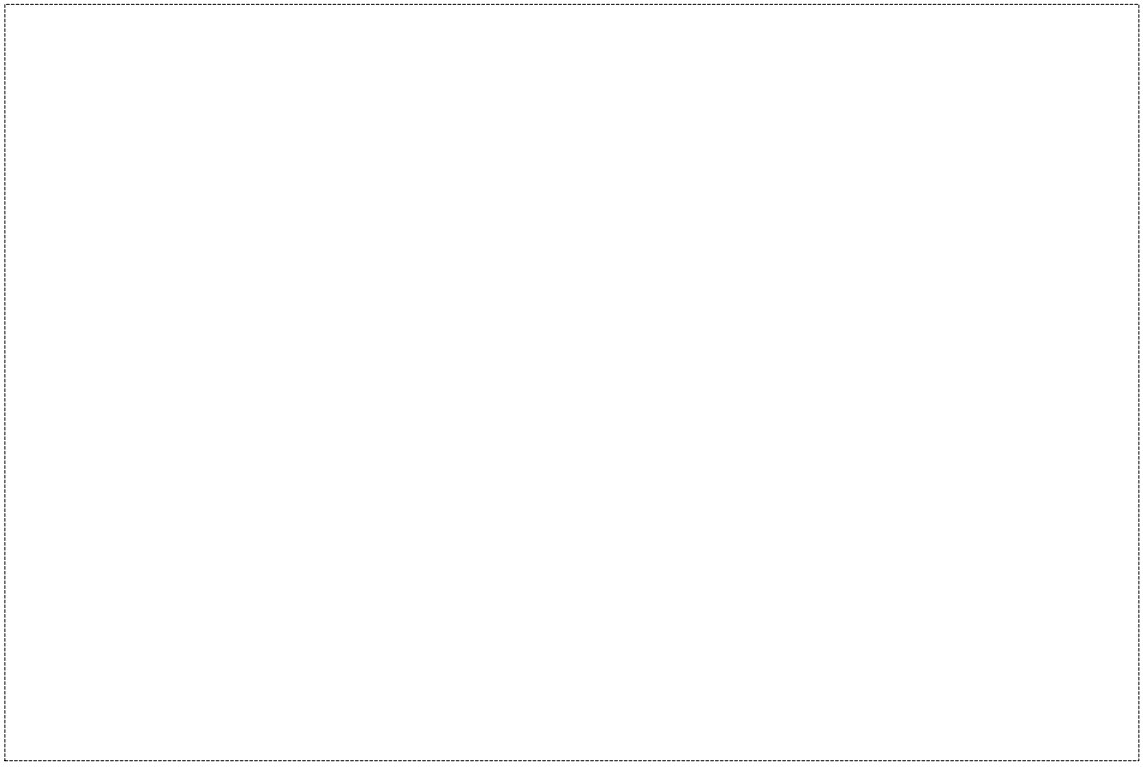

Fig. 2. Elastic angular distributions of neutron for aluminium from optimized optical potential parameters compared with measurements for energies up to 250 MeV

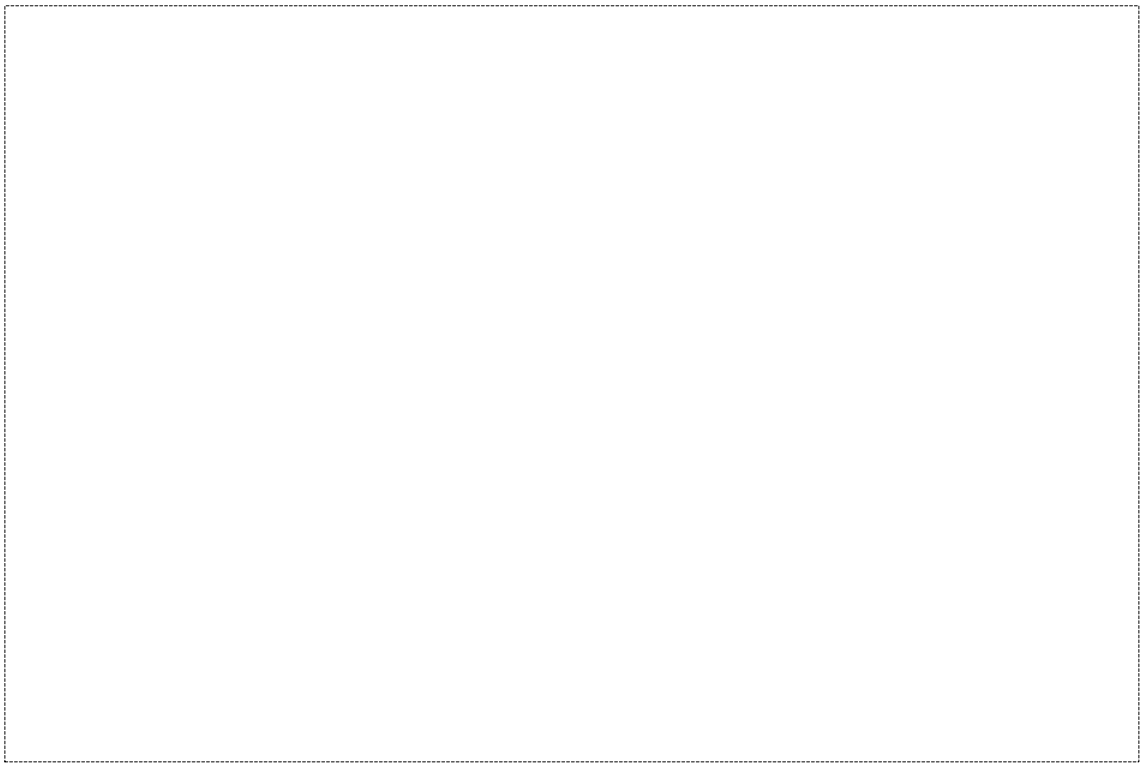

Fig. 3. Reaction sections of proton for aluminium from optimized optical potential parameters compared with measurements for energies up to 250 MeV

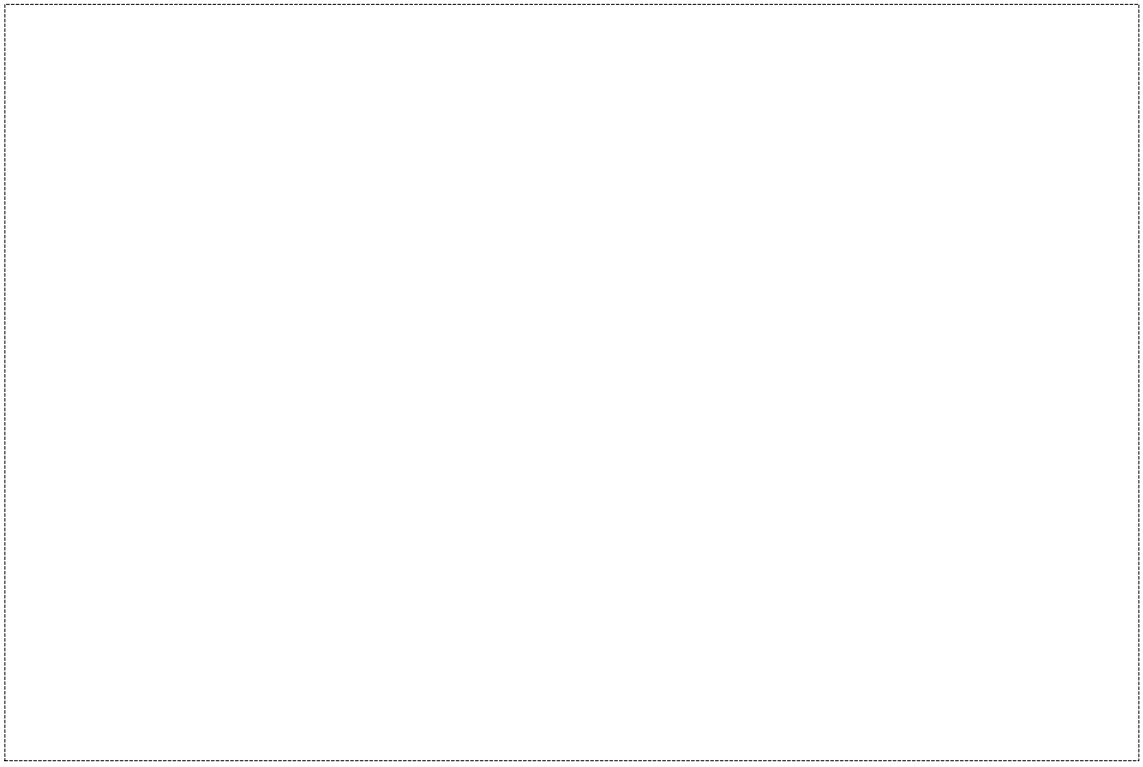

Fig. 4. Elastic angular distributions of proton for aluminium from optimized optical potential parameters compared with measurements for energies up to 250 MeV

Fig. 5. Evaluated Na-23 production cross sections of neutron for Al-27.
Reactions included:
(n,na), (n,dt), (n,npt), (n,n2d), (n,2npd), (n,3n2p), (n,n2d) (n,2npd) (n,3n2p)

Fig. 6. Evaluated Na-24 production cross sections of proton for Al-27.
Reactions included:
(p,2pd) (p,n3p)

Fig. 7. neutron emission spectra at 30 degree of 90 Mev (p,xn) reaction on Al-27

Fig. 8. Neutron total and reaction cross sections up to 2 GeV for Al-27

Fig. 9. Proton reaction cross sections up to 2 GeV for Al-27

Fig. 10. Neutron emission spectra from the reaction of proton (585 MeV) + Al-27 at different laboratory angles

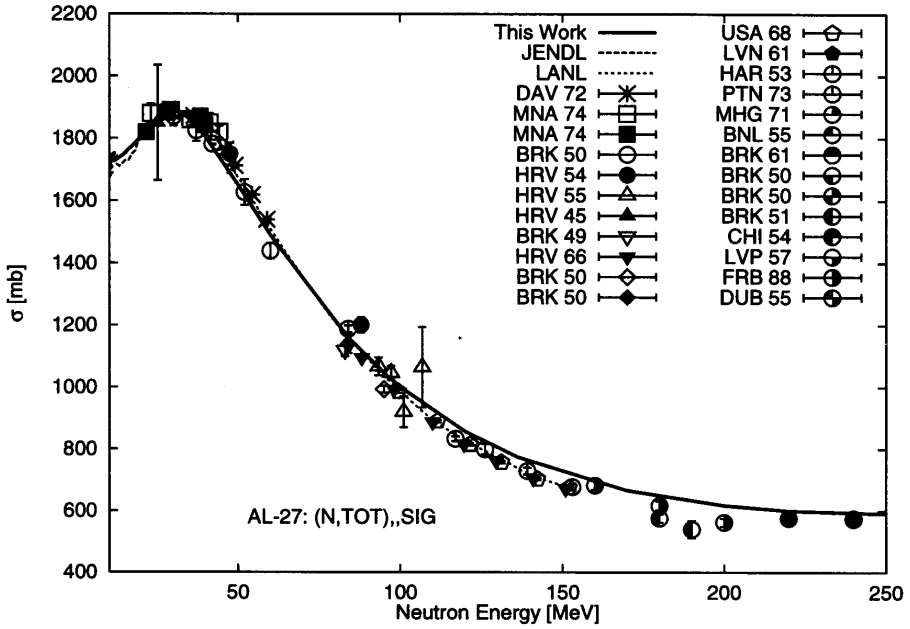

Fig. 1. Total cross sections of neutron for aluminium from optimized optical potential parameters compared with measurements for energies up to 250 MeV

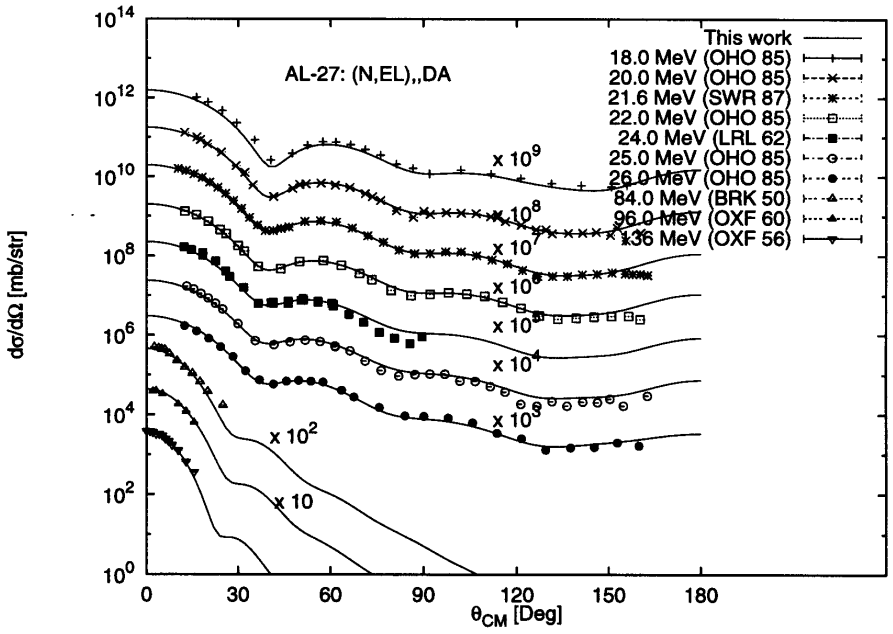

Fig. 2. Elastic angular distributions of neutron for aluminium from optimized optical potential parameters compared with measurements for energies up to 250 MeV

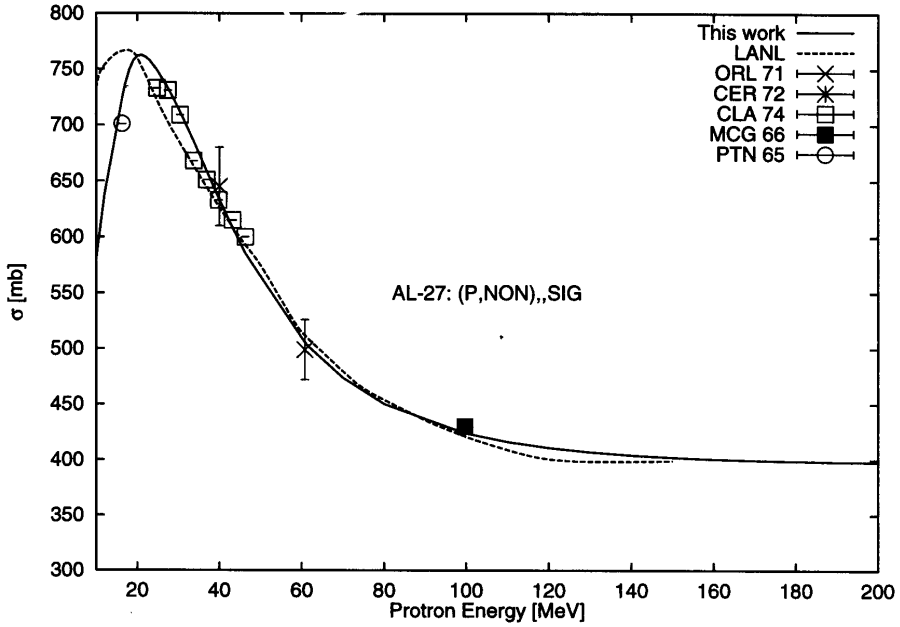

Fig. 3. Reaction sections of proton for aluminium from optimized optical potential parameters compared with measurements for energies up to 250 MeV

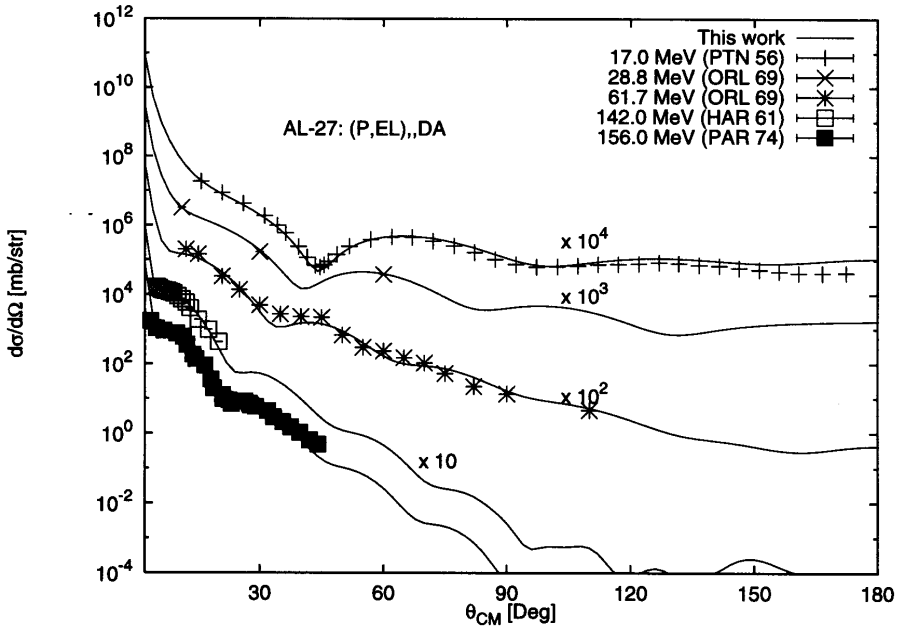

Fig. 4. Elastic angular distributions of proton for aluminium from optimized optical potential parameters compared with measurements for energies up to 250 MeV

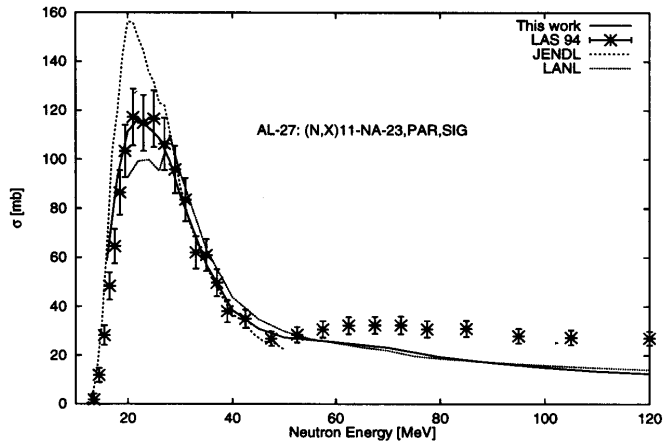

Fig. 5. Evaluated Na-23 production cross sections of neutron for Al-27.
Reactions included:
(n,na), (n,dt), (n,npt),
(n,n2d), (n,2npd), (n,3n2p),
(n,n2d) (n,2npd) (n,3n2p)

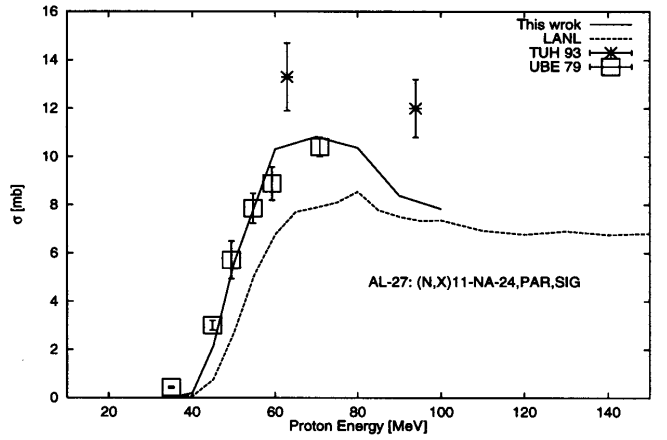

Fig. 6. Evaluated Na-24 production cross sections of proton for Al-27.
Reactions included:
(p,2pd) (p,n3p)

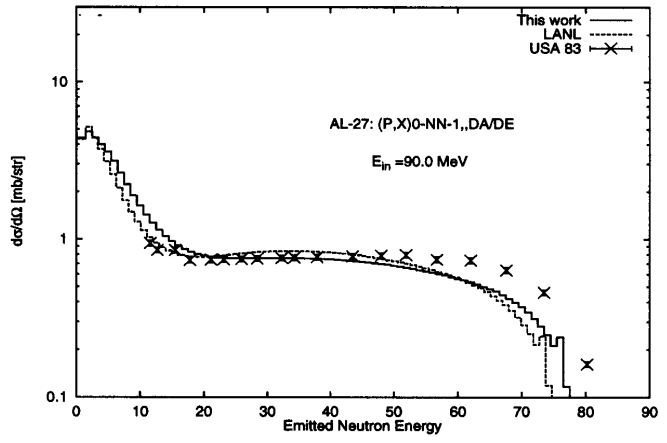

Fig. 7. neutron emission spectra at 30 degree of 90 Mev (p,xn) reaction on Al-27